2024 IEEE International Symposium on Mixed and Augmented Reality Adjunct (ISMAR-Adjunct) | 979-8-3315-0691-9/24/$31.00 ©2024 IEEE | DOI: 10.1109/ISMAR-Adjunct64951.2024.00134

Immersive Virtual Sculpting Experience with Elastoplastic Clay Simulation and Real-Time Haptic Feedback

Yang Gao Zhiyang Ji Peng Yu* Aimin Hao

State Key Laboratory of Virtual Reality Technology and Systems, Beihang University

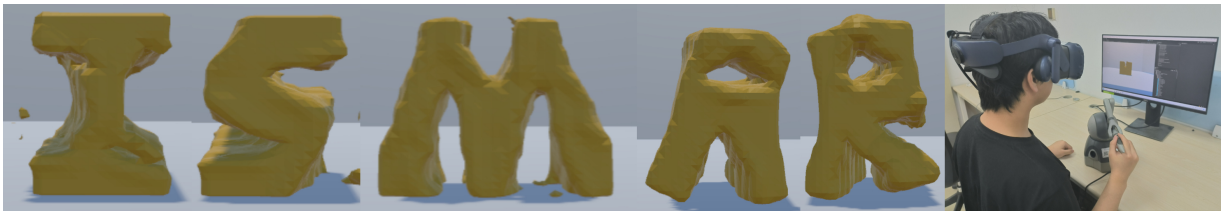

Figure 1: Immersive virtual sculpting with haptic feedback. Left: five carved letters "ISMAR". Right: A man wears a VR headset and engraves the virtual clay material by controlling the haptic device.

Abstract

Immersive virtual sculpting focuses primarily on geometric adjustments and ignores material properties and haptic feedback. This study enhances the sculpting experience by integrating physics-based elastoplastic materials and real-time haptic feedback. The key innovations include an advanced Material Point Method (MPM) for stable and accurate large-scale deformations, integrating material elasticity and plasticity. An improved haptic rendering algorithm calculates forces exerted by clay on the virtual tool and transmits them to the user, enhancing realism. An improved marching cubes algorithm enhances particle-mesh compatibility for better surface reconstruction. A controlled experiment with 52 participants demonstrated that our system increased task efficiency and performance compared to the control group, indicating a more immersive, tactile, and accurate sculpting experience.

Index Terms: Immersive virtual sculpting, elastoplasticity clay, haptics rendering.

1 Introduction

Virtual sculpting in VR environments has become essential for creating 3D assets and training artists. The rise of VR has enabled immersive 3D sculpting applications which provide intuitive environments yet often lack realistic material properties and tactile feedback. Innovative systems have aimed to simulate real-time human-computer interactions with realistic material properties. Studies have focused on simulating clay materials and stress feedback algorithms to enhance realism in virtual sculpting. For example, Barreiro et al. [2] used the Position-Based Fluid (PBF) method to simulate natural interactions with virtual clay. However, the material stiffness is dependent on the time step size and iteration counts. Meyer et al.[12] and Abdulali et al. [1] used the Finite Element Method (FEM) for elastoplastic materials, providing accuracy but high computational cost. The Material Point Method (MPM) has emerged as a powerful tool for simulating various materials, including elastic solids and particulate substances, offering superior collision management and handling of topology changes.

To create an integrated virtual sculpting experience, we used the MPM for clay deformation modeling and an enhanced Compatible Particle-In-Cell (CPIC) model for handling clay plasticity during virtual burin operations. Our improvements to the haptic rendering algorithm enhanced interaction force calculation, increasing immersion and realism. Post-cutting, a modified Marching Cubes (MC) algorithm updated the surface mesh using the signed distance field of the background mesh. At last, A controlled experiment demonstrated that our enhanced method improved task efficiency, and reduced cognitive loads, confirming the effectiveness of our integrated approach.

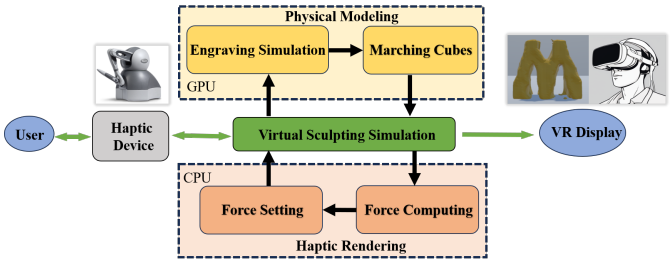

Figure 2: Our immersive virtual sculpting application framework allows users to control virtual sculpting via a haptic device, simulating elastoplastic deformation during engraving. An enhanced MC algorithm reconstructs the clay surface with improved accuracy. A haptic rendering algorithm computes the haptic force, and users monitor the process through a VR headset.

2 Related Work

2.1 Virtual Sculpting

Virtual sculpting is integrated into many 3D modeling applications which allow users to manipulate objects using hand controllers, emulating real-world sculpting. Despite advancements, these virtual models lack the tactile feedback of real materials. Valentini et al. [14] and Lu et al. [10] developed AR environments with haptic feedback, and Callens et al. [3] designed multi-layered devices for virtual object interaction. Nevertheless, these systems still fail to accurately replicate the physical properties of materials.Mandal et al. [11] used FEM-based volume meshes for haptic feedback but did not achieve real-time effects. Chen et al. [4] introduced a six-degree-of-freedom haptic system for actions like melting and burning, but without a physical volume model. This study emphasizes elastoplastic clay sculpting in VR, incorporating advanced methods

*e-mail:yupeng@buaa.edu.cn

2771-1110/24/$31.00 ©2024 IEEE
DOI 10.1109/ISMAR-Adjunct64951.2024.00134

for a realistic sculpting experience.

2.2 Physics Simulation

This paper focuses on viscoelastic clay and explores various physical modeling techniques in physics and computer graphics. FEM is often utilized for modeling elastic objects. Koschier et al. [9] developed a remeshing-free cutting algorithm using XFEM. However, it fails to address plastic deformation and are time-consuming for real-time virtual sculpting.PBF methods are preferred for real-time simulations due to their stability and performance. Barreiro et al. [2] used PBF for interaction with virtual clay . However, PBF methods lack physical accuracy as material stiffness depends on simulation time steps and iterations. The MPM approach can effectively simulates solid materials. Hu et al. [7] used a moving least-squares (MLS) approach to accelerate MPM and introduced CPIC for material cutting.In this paper, we proposed an improved MPM method to simulate clay, allowing interaction with a force-feedback-controlled virtual burin, incorporating elastoplastic deformation and CPIC-based cutting operations.

2.3 Haptic Rendering

Haptics rendering is crucial for sensing force, texture, material properties, and shape. The virtual coupling method is a widely used haptic rendering approach. Ortega et al.[13] introduced a six-degree-of-freedom "God Object" haptic rendering algorithm, where the virtual instrument's movement is constrainted to the object's surface, with haptic force calculated based on the positional difference between the God Object and the haptic device's proxy. Wang et al. [15] proposed a pose optimization function to align the God Object's pose with the haptic device's proxy, ensuring no intersection with the object.

In contrast, the virtual burin of virtual sculpting is capable of not only deforming the surface of a sculpted object through compression, but also cutting into the sculpting material. The virtual burin experiences pressure and friction during cutting, necessitating a real-time haptic rendering algorithm tailored for this application. Daviet et al.[5]'s Discrete Frictional Contact Problem (DFCP) involves inverting the Delassus operator, a computationally intensive process. This study proposes an innovative haptic rendering algorithm for virtual sculpting, enhancing realism and immersion by accurately modeling the forces experienced during sculpting tasks.

3 Method

Fig. 2 illustrates the software architecture of our system. The user operates the haptic device handle that controls the movement of the virtual burin. When the virtual burin collides with clay simulated on GPU based on the MLS-MPM method [7], the clay can deform and be cut apart according to section 3.1. At the same time, the force exerted on virtual burin is computed and set on the CPU according to Section 3.2. The surface of virtual clay is reconstructed using our improved MC algorithm, which is depicted in Section 3.3. Finally, the virtual sculpting scene is displayed in immersive VR environments.

3.1 Engraving Simulation

The MLS-MPM method integrates Lagrangian particles with Eulerian grids to solve continuum mechanics problems.Incorporating the moving least square method into MPM boosts performance over twofold. For more details, see [8] and [7].We propose an improvement based on MPM algorithm, which can combine elasticity and plasticity of physical materials reasonably.We adhere to [7] for notation, using p, q for particle indices and i, j for grid nodes.

The rigid virtual burin r represented as a triangle is discretized into an assemblage of particles. For each rigid particle r_η of r, the surrounding grid nodes $3\times3\times3$ are projected on the plane defined by $\mathscr{E}(r_\eta)$ and the signed distance between the points of

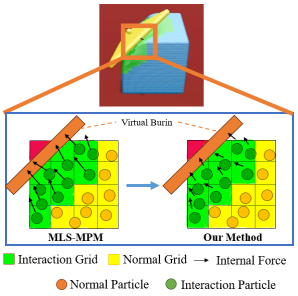

Figure 3: Comparison between our method and the traditional MLS-MPM method. The elastoplasticity of the clay becomes more apparent when squeezed with a burin.

the plane u_{i,r_η} is calculated. The minimum unsigned distance from the grid $\mathbf{x}_i$ to the virtual burin r is $d_i = \min_{r,\eta}|u_{i,r_\eta}|$. The tag $T_i = sign(u_{i,r_{\eta^*}(\mathbf{x}_i)})$ of grid node $\mathbf{x}_i$ is determined by the signed distance of the closest rigid particle $r_{\eta^*}(\mathbf{x}_i)$. The color information and the unsigned distance of the particles are reconstructed as T_p and d_p following [7]. The compatibility between the particle p and the grid node i is indicated as:

$$\delta_{i,p} = \begin{cases} 1, & T_p = 0 \vee T_i = 0 \vee T_p = T_i \\ 0, & \text{otherwise} \end{cases}. \tag{1}$$

In the P2G step, near rigid surfaces, particle information is only transferred to compatible grid nodes.

$$(m\mathbf{v})_i^n = \sum_p \delta_{i,p} w_{i,p} \left\{ m_p \mathbf{v}_p + \left[m_p \mathrm{C}_\mathrm{p}^\mathrm{n} - \mathrm{E}_\mathrm{p}^\mathrm{n} \right] \left(\mathbf{x}_i - \mathbf{x}_p^n \right) \right\}, \tag{2}$$

where m_i^n is computed as $m_i^n = \sum_p \delta_{i,p} w_{i,p} m_p$.The force impluse $\mathrm{E}_\mathrm{p}^\mathrm{n}$ delineated in Equation 2 proceeds as follows:

$$\mathrm{E}_\mathrm{p}^\mathrm{n} = \frac{4\Delta t}{\Delta x^2} \sum_p V_p^0 \zeta\left(d_p\right) \mathbf{P}(\mathbf{F}_\mathrm{p}^{\mathrm{n}+1})(\mathbf{F}_\mathrm{p}^{\mathrm{n}+1^\mathrm{T}}), \tag{3}$$

where Δt is the time step size, Δx is the grid size, V_p^0 is the undeformed vlome of partice p, $\mathbf{P}(\mathbf{F}_p^{n+1})$ is the first Piola-Kirchhoff (PK1) stress tensor. To model the elastoplasticity clay material, we proposed a function $\zeta\left(d_p\right)$:

$$\zeta\left(d_p\right) = \begin{cases} \frac{|d_p|}{3\Delta x}, & 0 < |d_p| \le 3\Delta x \\ 0, & otherwise \end{cases}. \tag{4}$$

This function $\zeta(d_p)$ linearly maps the distance d_p to a [0,1] interval, decreasing as d_p nears zero, signifying closeness to the interaction plane. A lower PK1 stress near zero d_p suggests a softer, more malleable materia.As shown in Fig. 3, when the virtual burin squeezes the virtual clay, the internal forces of the virtual clay are smaller than the elastic material modeled using the MLS-MPM method.

Particle advection. Following the traditional CPIC method, each particle contemporaneously updates its velocity and position and, in concordance with the CPIC methodology, modulates the magnitude of velocity commensurate with the proximity of the particle's location relative to the virtual burin.

3.2 Haptic Rendering

We propose a three-degree-of-freedom adaptation of the God-object method utilizing a penalty-based haptic rendering approach. As shown in Fig. 4, The spring force between the God-object and the virtual sculpting burin acts as the haptic force. Considering the interacting object as a rigid body, we focus only on translational

forces, ignoring torques. Surface changes in the clay affect the positions of the haptic and visual devices, indirectly influencing haptic force computation.

We use a constant π to determine if the God object is going to update its position.The constant π is defined as follows:

$$\pi = \begin{cases} 1, \sum_p (3\Delta x - d_p)|T_p| < \varepsilon \\ 0, otherwise \end{cases} \tag{5}$$

where ε is the minimum threshold measuring the number of rigid particles near the virtual burin, if there are enough particles around it, then π is set to 1, and the God object will stop updating its position. Otherwise, the God object will synchronize its position with that of the virtual burin.The procedural directive of the algorithm requires the additional documentation of an alternative pose, referred to as the virtual burin. The valuation of $\pi(\mathbf{x}_{rg})$ is ascertained in each frame. Upon attaining a denotation of 1, the virtual burin is rendered static. Otherwise, the virtual burin is refreshed to align with the displayed burin. The computation formula for the haptic force is as follows: $\mathbf{f} = k_h \cdot (\mathbf{x}_{rg} - \mathbf{x}_{ro})$, where k_h represents the stiffness coefficient of the spring model, $\mathbf{x}_{rg}$ represents the position of the God object, and $\mathbf{x}_{ro}$ represents the position of the virtual object.

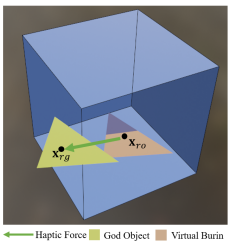

Figure 4: Haptic rendering illustration. The God object is constrained at the surface of virtual clay and the orange haptic device proxy is the virtual burin. A spring force between them is computed as the haptic force.

3.3 Improved Marching Cubes for Visual Rendering

The marching cubes algorithm is a widely used surface reconstruction approach for meshless objects. A background grid encloses the objects, and each grid node stores the unsigned density of the particles. The isosurface, where the unsigned density equals the given threshold, is the surface of objects. The isosurface of each cell of the background grid could be generated by searching the lookup table. The key is to compute the grid nodes' unsigned density of the particles.

As shown in the left image of Fig. 5, if we scatter particles' information to grid nodes without considering the compatibility $\delta_{i,p}$ between particle p and grid node i, we could not reconstruct a separated surface after burin cutting through the surface of the clay. The calculation of particle density should be influenced by the CPIC-derived chromatic interactions between particles and the grid. So, we proposed an innovative method to calculate $c_i = \sum_p \delta_{i,p} w_{i,p}$. The enhanced formulation affords the MC algorithm an augmented sensitivity in its response to the advent of separation planes engendered by actions such as rending and cleaving of objects, culminating in superior rendering outcomes.

4 Experiment and Validation

4.1 Implementation Details

We implemented our virtual sculpting system on a PC, which is equipped with an AMD R9-7800X3D processor operating at a frequency of 4.2 GHz, 64 GB memory, and NVIDIA RTX 4090 GPU. The haptic device is Geomagic Touch as shown in Fig. 2. The HTC Vive Pro2 is utilized for VR display.

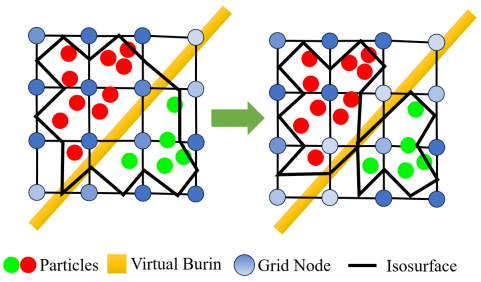

Figure 5: The traditional MC (left) can not reconstruct a separated isosurface like ours (right) after the virtual burin cutting through clay.

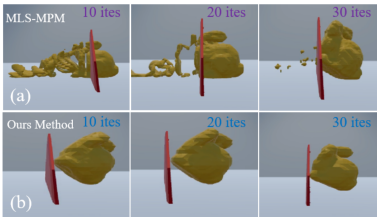

Figure 6: Visualizing the virtual burin's movement through bunny-shaped clay, with multiple iterations per frame, all within a 256^3 grid.

4.2 System Evaluation

To validate the effectiveness of our virtual sculpting system, we conducted an ablation study analyzing the impact of three enhancements on operational efficiency. We conducted the efficiency evaluation experiments under various conditions. In the worst-case scenario, our project achieved a 104.6% improvement in the time required for each physical computation compared to traditional methods[7], indicating relatively superior time performance. The system maintained a haptic rendering frame rate above 160, ensuring realistic haptic rendering.

The letters in Fig. 1 were engraved by the author within a six-minute timeframe.As shown in Fig. 6, the virtual burin's interaction with bunny-shaped clay material at various iterations per frame. Compared with the traditional MLS-MPM method, our approach, incorporating a ζ function, allowed for the plastic deformation of clay, preventing burin penetration through the material.

4.3 User Study

To evaluate the performance of our virtual sculpting system in the fields of cognition, emotion, and psychomotor, we conducted a controlled experiment utilizing the following three indicators: 1) Task completion time. 2) NASA Task Load Index (NASA-TLX) scale [6], used to measure workload. 3) The total score, which is calculated by the cumulative score for each user after quantifying the options on the NASA-TLX scale.

4.3.1 Participants

We recruited 52 participants, including 26 males and 26 females aged 20-30 (avg=22.35, std=3.93). Three participants were accustomed to using their left hand, while the others used their right hand. Before this experiment, We measured their experience with VR devices. Adhering to the principle of equal distribution, participants were assigned to the control or experimental group based on their experience with VR. The aim was to ensure a comparable level of VR experience and a number of genders between both groups. For the control group, participants completed virtual sculpting tasks using a traditional MLS-MPM based clay model and without haptic

feedback. For the experimental group, participants completed virtual sculpting tasks using our improved clay model and with haptic feedback.

4.3.2 Study Procedure

Participants familiarized themselves with VR and haptic devices before a sculpting task. The task is shaping a virtual clay cube into the letter 'M'. An exemplary task completion was shown to set objectives clearly.

After the task was completed, participants filled out the NASA-TLX scale to quantify perceived workload; responses yielded composite scores. Task completion status and time taken by both groups were documented for comparative analysis. A t-test compared mean values between groups, revealing statistically significant differences ($p < 0.05$) in self-reported performance, perceived effort, and frustration levels. See Tab. 1 for detailed results.

Table 1: The p-value and t-statistic of t-test in different dimensions.

Statistic / Dimensions	t-statistic	p-value
Mental Demands	.553	.584
Physical Demands	.653	.519
Temporal Demands	.850	.403
Self-reported Performance	-2.631	.014*
Effort	2.957	.006*
Frustration	2.060	.049*

* p-value < 0.05

5 Discussion

This study evaluated the practical application of the tools by analyzing users' subjective experiences before and after our optimization algorithms.

Performance Comparison. The experimental group showed significant performance improvements, reducing effort and frustration. Questionnaire results (Tab. 1) indicate significantly lower frustration in the experimental group compared to the control group ($p < 0.05$), and higher effort in the control group ($p < 0.01$). This confirms our methods enhance performance, reduce failure, and lessen mental exertion. The experimental group had a 32% reduction in average task completion time and significant self-evaluation improvements on the NASA-TLX scale ($p < 0.02, t < -2.6$). Total cognitive load was 19% lower in the experimental group, indicating easier and more effective task execution.

User Feedback. Control group users highlighted usability issues, especially the 'lack of haptic feedback,' leading to frustration. The experimental group suggested increasing the difficulty of the task and improving the virtual environment such as 'viewpoint control optimization' and 'increasing task difficulty.' This feedback supports the improved system's effectiveness in shifting user focus from simulation issues to task-related aspects.

6 Conclusion

This paper presents an immersive VR application for sculpting clay-like materials with haptic feedback. We utilized the MLS-MPM method for clay deformation and improved the CPIC method for handling elastoplasticity during sculpting with a virtual burin. To enhance realism, we introduced a three-degree-of-freedom haptic rendering algorithm that calculates and conveys spring forces to the operator through a haptic device. We also refined the MC algorithm for more accurate surface mesh generation. In a controlled experiment with 56 participants, the experimental group completed tasks faster and with lower psychological load scores, indicating our system's effectiveness in aiding virtual sculpting tasks. Despite its benefits, our method is limited by hardware performance, which affects simulation grid resolution and detail fidelity. We also plan to expand the scale and design different difficulty levels for these experiments soon, employing more diverse methods to evaluate the results. This will provide stronger evidence of the project's effectiveness.

Acknowledgments

This work was supported in part by the National Key R&D Program of China (no. 2023YFC3604500, 2023YFC3604505), the Postdoctoral Fellowship Program of CPSF under grant number GZC20233375, National Natural Science Foundation of China (L2324214, 62102036), Beijing Natural Science Foundation (L232102).

References

[1] A. Abdulali and S. Jeon. Data-driven haptic modeling of plastic flow via inverse reinforcement learning. In *2021 IEEE World Haptics Conference (WHC)*, pp. 115–120. IEEE, July 2021. 1

[2] H. Barreiro, J. Torres, and M. A. Otaduy. Natural tactile interaction with virtual clay. In *2021 IEEE World Haptics Conference (WHC)*, pp. 403–408. IEEE, July 2021. 1, 2

[3] E. Callens, F. Danieau, A. Costes, and P. Guillotel. A tangible surface for digital sculpting in virtual environments. In *Haptics: Science, Technology, and Applications: 11th International Conference, EuroHaptics 2018, Pisa, Italy, June 13-16, 2018, Proceedings, Part II 11*, pp. 157–168, 2018. 1

[4] H. Chen and H. Sun. Real-time haptic sculpting in virtual volume space. In *Proceedings of the ACM symposium on Virtual reality software and technology*, pp. 81–88, 2002. 1

[5] G. Daviet. Simple and scalable frictional contacts for thin nodal objects. *ACM Transactions on Graphics (TOG)*, 39(4):61–1, 2020. 2

[6] S. G. Hart and L. E. Staveland. Development of nasa-tlx (task load index): Results of empirical and theoretical research. In *Advances in psychology*, vol. 52, pp. 139–183. Elsevier, 1988. 3

[7] Y. Hu, Y. Fang, Z. Ge, Z. Qu, Y. Zhu, A. Pradhana, and C. Jiang. A moving least squares material point method with displacement discontinuity and two-way rigid body coupling. *ACM Transactions on Graphics (TOG)*, 37(4):1–14, 2018. 2, 3

[8] C. Jiang, C. Schroeder, J. Teran, A. Stomakhin, and A. Selle. The material point method for simulating continuum materials. In *Acm siggraph 2016 courses*, pp. 1–52. 2016. 2

[9] D. Koschier, J. Bender, and N. Thuerey. Robust extended finite elements for complex cutting of deformables. *ACM Trans. Graph.*, 36(4), jul 2017. 2

[10] P. Lu, B. Sheng, S. Luo, X. Jia, and W. Wu. Image-based non-photorealistic rendering for realtime virtual sculpting. *Multimedia tools and applications*, 74:9697–9714, 2015. 1

[11] A. Mandal, P. Chaudhuri, and S. Chaudhuri. Interactive physics-based virtual sculpting with haptic feedback. *Proceedings of the ACM on Computer Graphics and Interactive Techniques*, 5(1):1–20, 2022. 1

[12] K. A. Meyer, R. Skrypnyk, and M. Pletz. Efficient 3d finite element modeling of cyclic elasto-plastic rolling contact. *Tribology International*, 161:107053, 2021. 1

[13] M. Ortega, S. Redon, and S. Coquillart. A six degree-of-freedom god-object method for haptic display of rigid bodies with surface properties. *IEEE transactions on visualization and computer graphics*, 13(3):458–469, 2007. 2

[14] P. P. Valentini and M. E. Biancolini. Interactive sculpting using augmented-reality, mesh morphing, and force feedback: Force-feedback capabilities in an augmented reality environment. *IEEE Consumer Electronics Magazine*, 7(2):83–90, 2018. 1

[15] D. Wang, X. Zhao, Y. Shi, Y. Zhang, J. Hou, and J. Xiao. Six degree-of-freedom haptic simulation of probing dental caries within a narrow oral cavity. *IEEE transactions on haptics*, 9(2):279–291, 2016. 2